

## 6,4 - PP Photolyase Encoded by *AtUVR3* is Localized in Nuclei, Chloroplasts and Mitochondria and Its Expression is Down-Regulated by Light in a Photosynthesis-Dependent Manner

short title: **AtUVR3: localization and light regulated expression**

Agnieszka Katarzyna Banaś<sup>1,2</sup>, Paweł Hermanowicz<sup>1,2</sup>, Olga Sztatelman<sup>1,3</sup>, Justyna Łabuz<sup>1,2</sup>, Chhavi Aggarwal<sup>1,4</sup>, Piotr Zgłobicki<sup>1</sup>, Dominika Jagiełło-Flasińska<sup>1</sup>, Wojciech Strzałka<sup>1</sup>

<sup>1</sup> Department of Plant Biotechnology, Faculty of Biochemistry, Biophysics and Biotechnology, Jagiellonian University, Gronostajowa 7, Krakow, 30-387, Poland;

<sup>2</sup> The Malopolska Centre of Biotechnology, Jagiellonian University, Gronostajowa 7, Krakow, 30-387, Poland

<sup>3</sup> Institute of Biochemistry and Biophysics, Polish Academy of Sciences, 02-106 Warszawa, Poland

<sup>4</sup> Department of Gene Expression, Faculty of Biology, Adam Mickiewicz University, Poznan, 61-614, Poland

### Abbreviations:

BER - base excision repair

Col - ecotype Columbia

CPD - cyclobutane pyrimidine dimer

CRY - cryptochrome

DMSO - dimethyl sulfoxide

DSB - double strand break

eGFP - enhanced green fluorescent protein

*gl-1 - glabra 1*

HR - homologous recombination

H2B - histone 2B

*Ler* - ecotype Landsberg *erecta*

mRFP - monomeric red fluorescent protein

MMR - mismatch repair

NER - nucleotide excision repair

NES - nuclear export signals

NHEJ - nonhomologous end-joining

NIK - NF- $\kappa$ B-inducing kinase

NoLS - nucleolar localization signal

PARP - poly (ADP-ribose) polymerase

PHOT - phototropin

PHR1 - photoreactivating enzyme1

PHY - phytochrome

pNLS - putative nuclear localization signal

6-4 PP - pyrimidine-pyrimidone (6-4) photoproduct

PPFD - photosynthetic photon flux density

PTS1 - peroxisomal targeting signal1 (Ser-Lys-Leu)

SSB - single strand break

UVR2 - UV resistance2

UVR3 - UV repair defective3

UVR8 - UVB resistance 8

ZDP - zinc finger DNA 3'-phosphoesterase

**ABSTRACT**

Pyrimidine dimers are the most important DNA lesions induced by UVB irradiation. They can be repaired directly by photoreactivation or indirectly by the excision repair pathways. Photoreactivation is performed by photolyases, enzymes which bind to the dimers and use the energy of blue light or UVA to split bonds between adjacent pyrimidines. *Arabidopsis thaliana* has three known photolyases: AtPHR1, AtCRY3 and AtUVR3. Little is known about the cellular localization and regulation of AtUVR3 expression. We have found that its transcript level is down-regulated by light (red, blue or white) in a photosynthesis-dependent manner. The down-regulatory effect of red light is absent in mature leaves of *phyB* mutant, but present in leaves of *phyAphyB*. UVB irradiation does not increase *AtUVR3* expression in leaves. Transiently expressed AtUVR3-GFP is found in the nuclei, chloroplasts and mitochondria of *Nicotiana benthamiana* epidermal cells. In the nucleoplasm, AtUVR3-GFP is distributed uniformly, while in the nucleolus it forms speckles. Truncated AtUVR3 and mutants were used to identify the sequences responsible for its subcellular localization. Mitochondrial and chloroplast localization of AtUVR3 is independent of its N-terminal sequence. Amino acids located at the C-terminal loop of the protein are involved in its transport into chloroplasts and its retention inside the nucleolus.

**Keywords:** 6,4 - PP photolyase, AtUVR3, chloroplast, light regulated expression, mitochondria, nucleus.

## INTRODUCTION

Both environmental factors and metabolic processes can cause damage to genomic and organellar DNA. Sunlight, which contains mutagenic ultraviolet radiation (UV), can induce the formation of DNA lesions. The most dangerous UVC (100-280 nm) is absorbed in the atmosphere by the ozone layer. Only UVB (280-315 nm) and UVA (315-400 nm) affect plants under natural conditions. The indirect effects of UVB and UVA include ROS production, which promotes the formation of breaks in the DNA backbone (for a review see Rastogi et al. 2010). The most important direct effect of UVB is the formation of dimers between adjacent pyrimidines, mainly cyclobutane pyrimidine dimers (CPDs) and to a lesser extent pyrimidine-pyrimidone (6-4) photoproducts (6-4 PPs) (Friedberg et al. 1995). Under UVA, 6-4 PPs undergo isomerization into Dewar valence isomers. Its rate depends on the DNA sequence (Bucher et al. 2015).

Many DNA repair mechanisms have evolved in living organisms. Modifications of single bases, often induced by chemical mutagens, can be removed via excision repair mechanisms, including base excision repair (BER), nucleotide excision repair (NER) or mismatch repair (MMR). Double strand breaks (DSBs) are repaired mainly by nonhomologous end-joining (NHEJ) and less frequently by homologous recombination (HR, for a review see Waterworth et al. 2011). Single strand breaks (SSBs) are recognized by proteins belonging to the poly (ADP-ribose) polymerase (PARP) family. A set of enzymes also involved in BER repair is responsible for the repair of SSBs. In *Arabidopsis*, zinc finger DNA 3'-phosphoesterase (AtZDP) has been postulated to both recognize and repair SSBs (Petrucco et al. 2002).

In addition to indirect DNA repair mechanisms, pyrimidine dimers can be repaired in a single reaction called photoreactivation. This reaction is catalyzed by photolyases, enzymes which use the energy of blue light or UVA to directly split the bonds between neighbouring pyrimidines. Photolyases are found in most organisms, but not in placental mammals. They are specific to either CPDs or 6-4 PPs. To date, three *Arabidopsis* photolyases, AtPHR1 (photoreactivating enzyme1, UVR2 - UV resistance2), AtCRY3 (cryptochrome3) and AtUVR3 (UV repair defective3) have been characterized.

AtPHR1 is a CPD photolyase localized in the nucleus (Kaiser et al. 2009). It is present mainly in flowers, to a lesser extent in stems, and in a very low level in leaves and roots (Ahmad et al. 1997). The second *Arabidopsis* CPD photolyase is AtCRY3, localized in chloroplasts and mitochondria (Kleine et al. 2003). At first, this protein was reported to bind CPDs only in single stranded DNA (Selby and Sancar, 2006). It was postulated that it is

responsible for the photorepair of organellar DNA during transcription, when single stranded DNA loops are formed. However, the activity of AtCRY3 against CPD dimers has been demonstrated in double stranded DNA as well (Pokorny et al. 2008). The *Arabidopsis* mutant in the *AtUVR3* gene is defective in the photorepair of 6-4 PPs (Jiang et al. 1997, Nakajima et al. 1998). The photolyase activity of AtUVR3 has been shown *in vitro* (Nakajima et al. 1998). AtUVR3 has been found in all plant organs tested, with the highest level in siliques (Waterworth et al. 2002). Its subcellular localization has not been determined yet.

Photolyases are responsible for the repair of DNA damage induced by UV and require blue light for their activity, therefore one may expect that visible light or UV regulates their expression. Light can regulate gene expression through photoreceptor-dependent signaling pathways or photosynthesis-derived signals. The amount of *AtPHR1* mRNA increases under white light and this increase is greater when white light is supplemented with UVA or UVB (Ahmad et al. 1997, Tanaka et al. 2002, Castells et al. 2010). A more detailed examination was performed only recently using different spectral ranges and mutants of photoreceptors which absorb blue (cryptochromes (crys) and phototropins (photo)), red/far red (phytochromes (phys)) and UVB (UVB-RESISTANCE 8 (UVR8)). Each of the spectral ranges, blue, UVA and UVB can separately increase the *AtPHR1* transcript level. This regulation involves the cooperation of many pathways, but those activated by cryptochromes and UVR8 are the most important (Li et al. 2015). Data on the light/UV regulation of other *Arabidopsis* photolyases are scarce. Moldt et al. (2009) mentioned that the expression of *AtCRY3* was up-regulated by red light via the activation of phyA in etiolated *Arabidopsis* seedlings, but the experimental data were not shown. In etiolated seedlings, the *AtUVR3* transcript level slightly increased upon white light illumination (Castells et al., 2010).

As most previous studies have been devoted to CPD photolyases, the aim of this research was to characterize *AtUVR3*, an *Arabidopsis* 6-4 PPs photolyase, in more detail. The effect of light and UVB on the *AtUVR3* mRNA level was established and the involvement of photoreceptor- and photosynthesis-derived signals in its light regulation was examined. UVB irradiation can induce the formation of pyrimidine dimers in genomic and organellar DNA, thus the precise targeting of enzymes involved in DNA repair is crucial. Subcellular localizations of the full length *AtUVR3*, its mutants and truncated versions were determined. The obtained results revealed the presence of this protein in nuclei, chloroplasts and mitochondria and the role of its C-terminus in determination of subcellular localization.

## RESULTS

### The expression pattern of *AtUVR3*

Firstly, the expression pattern of *AtUVR3* in different organs of adult *Arabidopsis* plants, harvested in the middle of the day (i.e. 5 h after the onset of light), was examined. *AtUVR3* was detected in all organs tested. The transcript level differed between organs (one-way ANOVA  $F_{4,9}$  3.713,  $p$  0.0474). It was comparable in leaves, stems, and siliques, but it was lower in roots and in flowers (Fig. 1A). However, the differences between particular groups were not statistically significant when tested with Tukey's test.

The influence of UVB on the expression of *AtUVR3* in *Arabidopsis* WT and *uvr8-6* mutant was checked in rosette leaves of adult plants (Fig. 1B). After 3 h irradiation with  $0.2 \mu\text{mol}\cdot\text{m}^{-2}\cdot\text{s}^{-1}$  of UVB, the mRNA level was comparable with the dark control in both WT and *uvr8-6* leaves.

To establish the influence of light on the expression of *AtUVR3*, white light intensities in the range of  $100\text{--}500 \mu\text{mol}\cdot\text{m}^{-2}\cdot\text{s}^{-1}$  were applied for 3 h in experiments using dark-adapted mature *Arabidopsis* leaves (Supplementary Fig. S1A). The *AtUVR3* mRNA level was strongly down-regulated by light within the whole range of light intensities tested. White light of a chosen intensity ( $100 \mu\text{mol}\cdot\text{m}^{-2}\cdot\text{s}^{-1}$ ) down-regulated *AtUVR3* expression regardless of the duration of the treatment (from 1.5 h up to 24 h) (Supplementary Fig. S1B). A prolonged night (i.e. 16 h overnight dark adaptation plus 24 h in darkness) also reduced the mRNA level. 3 h illumination with white light of  $100 \mu\text{mol}\cdot\text{m}^{-2}\cdot\text{s}^{-1}$  ( $200 \mu\text{mol}\cdot\text{m}^{-2}\cdot\text{s}^{-1}$  for DCMU treatment) or red/blue light of  $50 \mu\text{mol}\cdot\text{m}^{-2}\cdot\text{s}^{-1}$  was chosen for the further experiments.

The light down-regulation of *AtUVR3* expression depended on the growth stage. Illumination with  $100 \mu\text{mol}\cdot\text{m}^{-2}\cdot\text{s}^{-1}$  of white light significantly decreased the *AtUVR3* level in mature leaves (decrease by 75%,  $p$  0.046), but it had only small and statistically insignificant effect on *AtUVR3* in aerial parts of 7-day-old seedlings (a decrease by 20%,  $p$  0.669) (Fig. 1C).

Light can control gene expression by either photoreceptor-activated signaling pathways or by photosynthesis-derived signals. DCMU, an inhibitor of photosynthesis, was used to distinguish between these routes (Fig. 1D). In control leaves, light strongly decreased the *AtUVR3* mRNA level (statistically significant,  $p$  0.00139). In DCMU pre-treated leaves, light caused a smaller decrease (statistically insignificant,  $p$  0.300). The effect of light on the *AtUVR3* level was reduced by DCMU, as further indicated by the significant interaction between light conditions and the presence/absence of DCMU (two-way ANOVA,  $F_{1,8}$  22.04,  $p$  0.00155). The presence of DCMU did not significantly influence the dark level of *AtUVR3* ( $p$  0.618).

To establish the involvement of photoreceptors in regulation of *AtUVR3* mRNA level, *Arabidopsis* wild type and photoreceptor mutants were used (Fig. 2A). Adult plants were illuminated with blue or red light to determine the light spectrum range involved in the process. Both blue and red light down-regulated *AtUVR3* expression in the wild type. In WT Columbia (Col), blue light decreased the *AtUVR3* level by 72%, while red light decreased it by 88%, as compared with the dark level. The dark *AtUVR3* level was the highest in Columbia (Col), while in Landsberg *erecta* (*Ler*) and *glabra-1* (*gl-1*) it was lower by 77% and 43%, respectively (Fig. 2A). The down-regulatory effect of red and blue light was preserved in all the photoreceptor mutants tested, apart from *phyB*, in which no red light induced down-regulation was observed (Fig. 2A). The lack of red light down-regulation in *phyB* was confirmed in a repeated experiment with three new biological replicates per group (Supplementary Fig. S2).

The effect of red and blue irradiation on the *AtUVR3* level was also examined in light-grown and etiolated 7-day-old seedlings (Fig. 2B). In light-grown WT *Ler* seedlings, the level of *AtUVR3* was significantly higher in darkened samples than in blue- or red-illuminated samples. The decrease of *AtUVR3* level after illumination was also observed in etiolated WT *Ler* seedlings, however, it was much smaller in magnitude and not statistically significant. A similar pattern was observed for the phytochrome mutants – in light-grown seedlings both red and blue illumination resulted in a substantial decrease of the *AtUVR3* level, statistically significant in all mutants except *phyA*, while in etiolated seedlings the effect of illumination was much smaller and statistically insignificant. Unlike leaves, *phyB* seedlings did not exhibit the altered response to red light (compare Fig. 2A and Fig. 2B). The magnitude of down-regulatory effect of red illumination observed in *phyB* was similar to that observed for WT *Ler* seedlings. Two-way ANOVAs, calculated separately for each plant line (WT *Ler/phyA/phyB/phyAphyB*), showed that the interaction between the growth conditions (etiolated/light-grown) and irradiation conditions (darkness/red/blue irradiation) was significant in all lines except *phyA* (WT *Ler*  $F_{2,12}$  9.747,  $p$  0.0031; *phyA*  $F_{2,12}$  0.132,  $p$  0.8776; *phyB*  $F_{2,10}$  9.699,  $p$  0.0046; *phyAphyB*  $F_{2,12}$  9.111,  $p$  0.0039).

### The subcellular localization of AtUVR3

The subcellular localization of AtUVR3 was examined using transient transformation with GFP-tagged proteins of *Nicotiana benthamiana* leaves. By far the brightest AtUVR3-GFP fluorescence was observed in the nucleus (Fig. 3A), weaker fluorescence was observed in mitochondria (Fig. 3B) and chloroplasts (Fig. 3C). No fluorescence was visible in the cytosol (Fig. 3D). In the nucleus, the fluorescence was especially bright in the circular region on the periphery of the nucleolus (Fig. 3A). The brightly fluorescent spot was often visible also in

the center of the nucleolus, giving it a bull eye appearance. A more uniform, less intensive signal was visible in the whole nucleoplasm. The fluorescence of GFP alone (i.e. the empty pK7WFG2 plasmid) was comparable in the nucleus and in the surrounding cytoplasm. It was uniform in the nucleoplasm, weaker in the nucleolus (Supplementary Fig. S3).

The co-transformation of AtUVR3-GFP with histone 2B fused with monomeric red fluorescent protein (mRFP) allowed to examine the co-localization of AtUVR3 with chromatin (Fig. 4A). In most nuclei, mRFP-H2B formed a bright ring on the edge of the nucleolus, where it co-localized with AtUVR3-GFP. However, in some nuclei the ring was not visible and mRFP fluorescence was present only in the nucleoplasm. The presence or absence of the histone 2B (H2B) ring seemed independent of its expression level. mRFP-H2B fluorescence in the nucleoplasm was mostly uniform, with a few brighter speckles visible. The red speckles usually co-localized with green speckles, visible in the AtUVR3-GFP channel (Fig. 4A).

AtUVR3-GFP fluorescence was also observed in cytoplasmic structures (Fig. 3B-C, Fig. 4B-C, Supplementary Fig. S4). In chloroplasts, the signal was non-uniform (Fig. 3C, Supplementary Fig. S4). Several brightly fluorescent spots (0.5 – 1  $\mu\text{m}$  in diameter) per chloroplast were often observed, with little signal in the remaining parts of the organelle. In some chloroplasts fluorescence was diffuse, but even in this case it was non-uniform, as non-fluorescent zones were observed. AtUVR3-GFP fluorescence was also observed in vesicle-like structures in the cytoplasm (Fig. 3B, Fig. Supplementary Fig. S4). To identify those structures, co-transformation with either peroxisomal targeting signal 1 (Ser-Lys-Leu) PTS1-mCherry, targeted to peroxisomes, or the N-terminal part cytochrome c oxidase IV fused to mCherry, targeted to mitochondria, was performed. Most of cytoplasmic AtUVR3-GFP co-localized with mitochondria (Fig. 4B). No co-localization with peroxisomes was observed (Fig. 4C).

Light did not influence the subcellular localization of AtUVR3-GFP transiently expressed in *Nicotiana* epidermis under the 35S promoter (Supplementary Fig. S4). Comparable fluorescence intensities and subcellular localizations of AtUVR3-GFP were observed in leaves left in darkness and those irradiated for 3 h with red or blue light of  $50 \mu\text{mol}\cdot\text{m}^{-2}\cdot\text{s}^{-1}$ , the same light intensities as used for the expression studies.

### Identification of the sequences responsible for subcellular localization of AtUVR3

The bioinformatical analysis of AtUVR3 amino acid sequence identified four amino acids (L96, S101, L104 and V105), which can potentially act as nuclear export signals (NESs) and three different nuclear localization signal (NLS) sequences (Fig. 5). These putative NLSs (pNLSs) include amino acids: 121-130 (pNLS1), 483-511

(pNLS2) and 509-537 (pNLS3). pNLS3 is a bipartite NLS (Fig. 5A, underlined), with a 23 amino acid spacer between two clusters of basic amino acids. To identify sequences responsible for the nuclear transport of AtUVR3 and its localization inside the nucleolus, muteins (Fig. 5A and Supplementary Fig. S5) and truncated versions of AtUVR3 protein (Fig. 5B) were used. In muteins, **basic residues, lysine and arginine (Fig. 5A, white letters K and R on a grey background)**, were substituted with alanine residues. The mutated sequences were marked from m1 up to m4. The substitution m1 was in the first, m2 in the second and the third, m3 and m4 in the third pNLS sequence (Fig. 5A). Amino acids present in truncated proteins (Fig. 5B) were denoted by a subscript. The subcellular localization of truncated AtUVR3-GFP forms and muteins was observed in epidermal cells of transiently transformed *Nicotiana benthamiana*. AtUVR3<sub>(1-501)</sub>-GFP, lacking the last helix, was localized in the nucleus (Fig. 6A) and mitochondria (Fig. 6B-C). However, it seemed to be less efficiently transported into the nucleus, as the ratio of nuclear fluorescence to that of the surrounding cytoplasm was smaller than in the case of the full-length protein (compare Fig. 3D and Fig. 6E). The fluorescence of AtUVR3<sub>(1-501)</sub>-GFP was much weaker in the chloroplasts than in the surrounding cytoplasm (Fig. 6D). The subcellular localization of AtUVR<sub>(122-556)</sub>-GFP, lacking the N-terminal part with pNLS1, was the same as the localization of wild type AtUVR3-GFP (compare Fig. 3 and Fig. 7). AtUVR<sub>(122-556)</sub>-GFP was present in the nucleus. It was uniformly localized in the nucleoplasm with visible retention in the nucleolus (Fig. 7A). It was also present in mitochondria (Fig. 7B-C) and chloroplasts (Fig. 7D). Muteins AtUVR3.m1-GFP, AtUVR3.m2-GFP and AtUVR3.m3-GFP were found in **and the nucleus (Fig. 8), chloroplasts (Fig. 9) and mitochondria (Fig. 10)**. AtUVR3.m4-GFP was present only in the nucleus and mitochondria. All proteins with mutations in amino acids 535-537 (.m4; .m24; .m34; .m234) were absent from chloroplasts (Fig. 9). They were also less efficiently transported into nuclei and mitochondria, with a significant amount of the protein remaining in the cytoplasm (Fig. 8 and Fig. 10, Supplementary Fig. S6). In some cells exclusion zones were observed in the place of mitochondria.

### Identification of amino acids responsible for intranuclear localization of AtUVR3

As mentioned above, wild type AtUVR3-GFP and the protein without the first 121 amino acids (AtUVR3<sub>(122-556)</sub>-GFP) were localized uniformly in the nucleoplasm and enriched in the nucleolus (Fig. 3A, Fig. 4A and Fig. 7A). Truncated AtUVR3 without the last 55 amino acids was localized only in the nucleoplasm outside the nucleolus (Fig. 6A). The role of specific amino acids in the nucleolar localization of this photolyase was examined using muteins. Strong retention in the nucleolus was observed for wild type AtUVR3-GFP and for AtUVR3.m1-GFP (Fig. 8). Several muteins, including AtUVR3.m2-GFP and AtUVR3.m34-GFP showed a decrease in the

nucleolar signal as compared with the wild type. AtUVR3.m234-GFP, in which lysine and arginine residues in pNLS2 and pNLS3 were substituted with alanine residues, was present in the nucleoplasm, but absent from the nucleolus (Fig. 8).

## DISCUSSION

### Down-regulation of the *AtUVR3* expression by light

Initially, it was reported that mRNA of *AtUVR3* was undetectable in 4-week-old leaves, roots and stems. It was present in low levels in flower buds and 2-week-old stem meristems (Liu et al. 2000), but light conditions were not specified. Subsequently, the highest level of the AtUVR3 protein was found in siliques, lower in flowers and 2- and 5-week-old leaves. It was not found in roots. The protein level did not increase after exposure to white light (up to 8 h of light after 24 h of dark) or UVB (Waterworth et al. 2002). An opposite effect of light was observed in etiolated *Arabidopsis* seedlings, where white light of  $200 \mu\text{mol}\cdot\text{m}^{-2}\cdot\text{s}^{-1}$  applied for 1 h doubled the *AtUVR3* transcript level (Castells et al. 2010).

We found that the *AtUVR3* transcript was present in all organs tested, including roots. We also observed significant light-dependent down-regulation of the *AtUVR3* mRNA expression (Fig. 1, Fig. 2A, Supplementary Fig. S1) in mature leaves. This strong white light regulation was not present in 7-day-old seedlings (Fig. 1B) indicating that it depends on the growth stage.

The high level of *AtUVR3* transcript under dark conditions is in line with the immediate 6-4 PPs photorepair in dark-adapted plants (Waterworth et al. 2002, Tanaka et al. 2002). By contrast, the CPD dimer removal is delayed, which is probably caused by a very low dark level of both the mRNA and protein encoded by *AtPHR1*. Light up-regulates *AtPHR1* expression, but this process takes time (Waterworth et al. 2002, Li et al. 2015). We may speculate that the accumulation of the *AtUVR3* transcript in darkness results in a higher protein level, so that the repair of 6-4 PPs can start immediately after turning on the light. The physiological role of the down-regulation of the expression of a light-activated enzyme is intriguing. UV irradiation causes formation mainly of CPD dimers, and to a lesser extent 6-4 PPs (Friedberg et al. 1995). Thus, the level of the CPD photolyase seems to be more important for plant survival. AtPHR1, the CPD photolyase, is produced when light is switched on (Waterworth et al. 2002, Li et al. 2015). Accumulation of AtUVR3 responsible for the repair of 6-4 PPs during the night may be less energy-consuming than keeping its level high constantly.

*AtUVR3* expression is down regulated by both blue and red light, which suggests that its regulation depends either on photosynthesis derived signals, a photoreceptor absorbing both red and blue light or a network of blue and red light photoreceptors. The experiments performed using DCMU imply that photosynthesis-derived retrograde signals from chloroplasts to the nucleus are involved in the *AtUVR3* level regulation (Fig. 1D). Thus, *AtUVR3* production is inhibited during the day, as long as photosynthesis is undisturbed. High, DNA-damaging UVB doses (inducing among others 6-4 PPs, which can be repaired by *AtUVR3*) impair also photosynthesis.

Weak down-regulation of *AtUVR3* levels by both blue and red light in etiolated seedlings contrasted with a pronounced down-regulatory effect observed in light-grown seedlings (Fig. 2B). The photosynthetic machinery in etiolated seedlings does not fully develop until they are exposed to light. The weak effect of light on the *AtUVR3* level in etiolated seedlings supports the hypothesis that chloroplasts control its expression.

A series of experiments with photoreceptor mutants confirmed that neither cryptochromes nor phototropins are involved in the control of *AtUVR3* mRNA levels in leaves (Fig. 2A). However, red light did not affect *AtUVR3* transcript level in the *phyB* mutant (Fig. 2A, Supplementary Fig. S2). Light down-regulated *AtUVR3* in the *phyAphyB* mutant, so the retrograde signal responsible for down-regulation of the *AtUVR3* mRNA level is generated independently of *phyA* and *phyB*. It seems that in the absence of *phyB*, *phyA* affects the transduction of the signal. This effect of *phyA* depends on the growth stage, as it was not observed in seedlings (compare Fig. 2A and Fig. 2B). Antagonistic action of *phyA* and *phyB* has been observed at different life stages during seedling photomorphogenesis, their shade avoidance and plant flowering (Whitelam et al. 2003, Devlin et al. 2003, Valverde et al. 2004). The interplay between phytochromes and retrograde signaling during seedling photomorphogenesis has been shown recently (Martin et al. 2016). Our results suggest similar interactions in adult plants (Fig. 2A). The mechanism of such interplay is unknown. *phyA*-regulated (SORLREP3) and *phyA*-associated (SORLREP2) sequences are found in the *AtUVR3* promoter (Hudson and Quail 2003, AGRIS database, <http://arabidopsis.med.ohio-state.edu/>). Thus, we can speculate that a transcription factor controlled by *phyA* or *phyA* itself binds to the *AtUVR3* promoter in the absence of *phyB*. In consequence, the retrograde-dependent inhibition of *AtUVR3* expression is blocked. Alternatively, *phyA*-activated processes may influence the stability of *AtUVR3* mRNA.

The impact of photosynthesis on UV sensitivity in a circadian clock-independent manner has been shown in *Chlamydomonas reinhardtii* (Chaudhari et al. 2015). The production of DSBs in plastid DNA has induced plastid-to-nucleus retrograde signaling, regulating the expression of many nuclear genes (Lepage et al. 2013). However, this is not the case for *AtUVR3*, as irradiation with UVB, which indirectly leads to the formation of

DSBs, did not up-regulate its mRNA level (Fig. 2B). It seems that photosynthetic performance alone is an indicator of the need for further production of AtUVR3.

### **Nuclear, mitochondrial and chloroplast localization of AtUVR3**

6-4 PPs are efficiently removed from total *Arabidopsis* DNA, including nuclear DNA (Chen et al. 1996, Draper and Hays, 2000). AtUVR3 is predicted to localize in the nucleus, mitochondria, chloroplasts or even extracellularly according to the The SubCellular Proteomic Database (Tanz et al. 2013). In the present study, the AtUVR3-GFP fusion protein was shown to localize in all DNA containing organelles - the nucleus, chloroplasts and mitochondria (Fig. 3 and Fig. 4). This triple location was not affected by light conditions (Supplementary Fig. S4), although light strongly reduced the *AtUVR3* mRNA level in mature *A. thaliana* leaves (Fig 2A).

AtUVR3-GFP was observed predominantly in the nucleus (Fig. 3A, D). The nuclear localization of AtUVR3-GFP did not result from passive diffusion, as the fluorescence of AtUVR3-GFP was very low in the cytoplasm surrounding the nucleus (Fig. 3 D). By contrast, GFP (expressed alone) was present in the cytoplasm and the nucleus in similar concentration (Fig. 3 D). Passive transport of AtUVR3-GFP is unlikely also due to its relatively high molecular mass of ca. 91 kDa. The fluorescence of AtUVR3-GFP was brightest in the nucleolus, while fluorescence of GFP alone was weaker in the nucleolus than in the nucleoplasm. This suggests that the nucleolar localization was specific to AtUVR3, not to the GFP tag. All truncated forms of AtUVR3 and its muteins were transported into nuclei (compare cell overviews in Fig. 3, Fig. 6 - 7 and Fig. S6), but those lacking the C-terminal amino acids and those with altered charge of the last helix (i.e. substitution of lysines/arginines to alanines in .m4, .m24, .m34 and .m234) were also present in the cytoplasm (compare AtUVR3 - Fig. 3, AtUVR3<sub>(1-501)</sub> - Fig. 6 and AtUVR.m4, .m24, .m34, .m234 - Supplementary Fig. S6). The C-terminal part of the protein is also important for chloroplast and mitochondrial localization of AtUVR3. Muteins with lysines/arginines substituted in positions 535-537 with alanines (.m4, .m24, .m34 and .m234) were less efficiently transported into mitochondria and were not found in chloroplasts (Fig. 8, Fig. 9). In addition, lack of last helix in AtUVR3<sub>(1-501)</sub>-GFP impaired its transport to chloroplasts (Fig. 6).

The presence of AtUVR3<sub>(122-556)</sub>-GFP, without the first 121 amino acids, in chloroplasts and mitochondria suggests that it can be transported to these organelles in a manner independent of its N-terminus (Fig. 7). Most of nuclear-encoded chloroplast proteins have an N-terminal transit peptide, but some of them lack it (Armbruster et al. 2009, Jarvis 2008). They have either an internal targeting signal or use the ER-Golgi pathway. The lack of the

transit peptide and the importance of the C-terminal part for organellar localization has been shown recently for the rice CPD photolyase (Takahashi et al. 2014).

The data on the photorepair activity in *Arabidopsis* organelles are ambiguous. CPD dimers were efficiently repaired in nuclear DNA of 5-day-old *Ler transparent testa-5* seedlings illuminated with white light following UV irradiation (Chen et al. 1996). Almost no repair was observed in mitochondrial or chloroplast DNA of these seedlings. However, CPDs were efficiently removed from chloroplast and mitochondrial DNA of mature *Arabidopsis* leaves under blue light, but not in darkness (Draper and Hays, 2000), which indicates the involvement of a photolyase. Thus, the CPD photorepair activity in *Arabidopsis* organelles may depend on the plant age. Photorepair of 6-4 PPs in plant organelles has not been tested yet. The localization of AtUVR3 in nuclei, chloroplasts and mitochondria suggests that it is involved in the DNA repair in the whole cell. Similar triple localization has been shown for the rice CPD photolyase (Takahashi et al. 2011).

#### **In the nucleus AtUVR3 is localized in the nucleoplasm and is enriched in the nucleolus**

The nucleolus is widely described as a place of ribosome assembly. However, proteins responsible for maintaining chromatin structure, mRNA metabolism and translation have also been found in the nucleolome (i.e. nucleolar proteome) of animal cells (Antoniali et al. 2014). The animal nucleolus contains proteins involved in DNA repair via NER, BER, SSB and DSB repair specific pathways (Antoniali et al. 2014, Ogawa and Baserga 2017). The data on the plant nucleolome are scarce. To date, 217 proteins have been annotated in the Arabidopsis Nucleolar Protein Database (AtNoPDB Database, <http://bioinf.scri.sari.ac.uk/cgi-bin/atnopdb/home>, Brown et al. 2005), but none of them is involved in DNA repair. This database is based on the results obtained by Pendle et al. (2005), who isolated nucleoli from the suspension culture of *Arabidopsis thaliana*, ecotype *Ler*. According to NoD (Nucleolar localization sequence detector, <http://www.compbio.dundee.ac.uk/www-nod/index.jsp>), AtUVR3 does not have any nucleolar localization signals (NoLS). The overall charge of C-terminus of AtUVR3 seems to be important for its retention in the nucleolus (compare wild type AtUVR3, .m1 and .m234 in Fig. 8 and AtUVR3<sub>(1-501)</sub> in Fig. 6). A role of charged regions in protein retention inside the nucleolus has been demonstrated for NF- $\kappa$ B-inducing kinase (NIK) and HIV-1 Tat (Musinova et al. 2015).

In the nucleus AtUVR3 co-localized with H2B, the core histone (Fig. 4A). H2B has been found in the *Arabidopsis* nucleolome (Pendle et al. 2005). However, when transiently expressed in fusion with fluorescent proteins, it has been detected inside (Wege et al. 2016) or outside the nucleolus (Martin et al. 2009, Crivelli et al. 2011, Gushchin et al. 2013, Rossi et al. 2014). We observed H2B either inside or outside the nucleolus in

neighboring cells (compare Fig. 4A and lower panel - an overview). Nucleolar localization of H2B seemed to be independent of its expression level. Still unidentified factors are responsible for H2B retention in the nucleolus.

## MATERIALS AND METHODS

### Bioinformatic analysis

*In silico* analysis of putative amino acids involved in AtUVR3 nuclear localization was performed using NucPred (<http://www.sbc.su.se/~maccallr/nucpred/>, Brameier et al. 2007) and cNLS Mapper ([http://nls-mapper.iab.keio.ac.jp/cgi-bin/NLS\\_Mapper\\_form.cgi](http://nls-mapper.iab.keio.ac.jp/cgi-bin/NLS_Mapper_form.cgi), Kosugi et al. 2009). Amino acids which serve as Nuclear Export Signals (NES) were predicted using NetNES1 (<http://www.cbs.dtu.dk/services/NetNES/>, la Cour et al. 2004). The AtUVR3 model (PDB 3FY4) was prepared using Polyview 3D (Porollo and Meller, 2007) based on the structure obtained with X-Ray diffraction (Hitomi et al., 2009). The protein chain was rendered using PyMol.

### Plant material and culture conditions

Seeds of *A. thaliana* wild-type ecotype Columbia (Col), *glabra-1* (*gl-1*) and Landsberg *erecta* (*Ler*), phytochrome (*phyA*, *phyB*, *phyAphyB*) and *uvr8-6* (SALK\_033468, Favory et al. 2009), *phot1* (SALK\_088841 Lehmann et al., 2011) mutants were purchased from Nottingham Arabidopsis Stock Centre (Nottingham, UK). Seeds of *phot2*, *phot1phot2* and cryptochrome mutants were a kind gift from J. Jarillo, Instituto Nacional de Investigación y Tecnología Agraria y Alimentaria, Madrid, Spain, Anthony R. Cashmore, Plant Science Institute, Department of Biology, University of Pennsylvania, Philadelphia, USA and Chentao Lin, University of Illinois, Chicago, USA, respectively. Phytochrome mutants were *Ler* background; *uvr8-6*, cryptochrome and phototropin single *phot1* and *phot2* mutants were Col background. The genetic background of the double *phot1phot2* mutant was Col, *gl-1*. If not stated otherwise, ecotype Col was used in the experiments. For the experiments with adult plants, *Arabidopsis* was grown in Jiffy-7 pots (Jiffy Products International AS) in a growth chamber (Sanyo MLR 350H) at 23 °C, 80% relative humidity, with a photoperiod of 10 h light and 14 h darkness, at 70-100  $\mu\text{mol m}^{-2} \text{s}^{-1}$  PPFD supplied by Sanyo FL40SS.W/37 lamps. For the experiments with seedlings, the seeds were surface sterilized and sown on B5 medium with 1% sucrose, solidified with 0.7% agar. After 2-day stratification in a cold room they were grown in a phytotron room at 23°C, with a photoperiod of 10 h light and 14 h darkness, at 60-70  $\mu\text{mol m}^{-2} \text{s}^{-1}$  PPFD supplied by Sanyo FL40SS.W/37 lamps. In the case of etiolated seedlings, after

sowing the plates were wrapped in aluminium foil, put into a black box, stratified in a cold room for 2 days and kept in the phytotron.

*Nicotiana benthamiana* plants were grown for three weeks in Jiffy pots in a culture chamber under the same conditions as *Arabidopsis* plants, transplanted into individual pots with universal commercial soil (COMPO SANA, Compo, Poland) and transferred into a phytotron (with a photoperiod of 10 h light and 14 h darkness, at 70-80  $\mu\text{mol m}^{-2} \text{s}^{-1}$  PPFD supplied by Tops 10 Power Pure White Led OSW4XAHAE1E) for additional four weeks.

### Experimental treatments

Dark adaptation started at the point when the day phase ended in the culture chamber.

*The effect of white light on the AtUVR3 transcript levels in seedlings and leaves.* 7-day-old seedlings and 5-week-old *Arabidopsis* plants were dark adapted for 16 h. The treatment group seedlings and mature plants were then irradiated for 3 h with white LED light of 100  $\mu\text{mol}\cdot\text{m}^{-2}\cdot\text{s}^{-1}$  (Tops 10 Power Pure White Led OSW4XAHAE1E), while the control groups were kept in darkness. The aerial parts of the seedlings and rosette leaves were then harvested and frozen in liquid nitrogen.

*Levels of AtUVR3 in different organs.* Roots, leaves, siliques, flowers and stems were harvested from soil-grown flowering *Arabidopsis* plants (at least 8-week-old) and frozen in liquid nitrogen. The material was collected in the middle of the day (5 h after the onset of light, at the same daytime when the 3 h illumination of samples used for testing involvement of light on the *AtUVR3* expression was completed).

*The involvement of photosynthesis in the light regulation of gene expression.* Mature leaves on 5-week-old *Arabidopsis* plants were treated with 200  $\mu\text{M}$  DCMU (Diuron, Sigma-Aldrich) in 0.4% dimethyl sulfoxide (DMSO) solution or 0.4 % DMSO alone as a control (see Łabuz et al. 2012). The plants were kept in darkness for 16 h. Plants allocated to the treatment group were then irradiated for 3 h with white light of 200  $\mu\text{mol}\cdot\text{m}^{-2}\cdot\text{s}^{-1}$  in a growth chamber (Fytoscope FS130 Photon System Instruments, equipped with W42180 - pure white LEDs), while the control plants were kept in darkness.

*The effect of light on AtUVR3 levels in Arabidopsis photoreceptor mutants.* Whole 5-week-old *Arabidopsis* plants were dark-adapted for 16 h and then irradiated for 3 h with blue (470 nm) or red (660 nm) LED light of 50  $\mu\text{mol}\cdot\text{m}^{-2}\cdot\text{s}^{-1}$ . The control plants were at that time kept in darkness. Rosette leaves were then harvested and frozen in liquid nitrogen. The same light treatments were applied for 7-day-old etiolated or light-grown phytochrome mutant and WT seedlings.

*The effect of UVB on the AtUVR3 transcript levels.* Whole WT and *uvr8*, 5-week-old *Arabidopsis* plants were dark adapted for 16 h. The treatment group plants were then irradiated with UVB of  $0.2 \mu\text{mol}\cdot\text{m}^{-2}\cdot\text{s}^{-1}$ , obtained using the WG305 cut-off filters in a custom-made growth chamber, equipped with USHIO UV-B Lamps G8T5E (see Sztatelman et al. 2015), while the control plants were kept in darkness. Rosette leaves were then harvested and frozen in liquid nitrogen.

*RNA isolation and real-time PCR.* Total RNA was isolated with the Spectrum™ Plant Total RNA Kit (Sigma-Aldrich). DNA was digested on a column according to the manufacturer's protocol (Sigma-Aldrich). mRNA was reverse transcribed using the RevertAid M-MuLV Reverse Transcriptase Kit (Thermo Scientific) with oligo(dT)<sub>18</sub> primers. Real-time PCR experiments were performed as in Łabuz et al. 2012, with all reactions run in triplicates. The primer sequences of reference genes: *PDF2*, *SAND*, *UBC* and *UBQ10* based on Czechowski et al. (2005) and of *AtUVR3* based on Castells et al. 2010 are listed in Supplementary Table S1. *PDF2*, *SAND* and *UBC* were used as reference genes in experiments with photoreceptor mutants and DCMU. In the rest of experiments *UBQ10*, *PDF2*, *SAND* and *UBC* were used as reference genes. Typically, three biological replicates were performed for each experimental group. In the experiments on the effect of UVB, six biological replicates per group were used. In the experiments with different light intensities and illumination times one biological replicate, consisting of leaves pooled from 10 plants, was used for each light intensity or illumination time. In all experiments, cDNA from different treatment groups was pooled together and used as the reference for calculating relative expression levels. Statistical analysis was performed on log-transformed relative expression levels, normalized to the geometric mean of the reference gene levels (Vandesompele et al 2002). The statistical significance of treatment effects was assessed with one- or two-way (as specified in the text) ANOVA, followed by Student's test (for two-level factors) or Dunnett's test (if more levels). Tukey's test was used for pairwise comparison of the mean transcript level in organs. All statistical calculations were performed using the R software.

*Preparation of plasmids and the transient transformation of Nicotiana benthamiana.* The *AtUVR3* coding sequence was cloned from cDNA prepared from mature *Arabidopsis* leaves. The Gateway technology (Invitrogen) was used to obtain 35S-*AtUVR3*-(full length/fragments/mutants)-GFP constructs in the pK7FWG2 destination vector. The overview of the pNLS fragments of *AtUVR3* and *AtUVR3* mutants used is shown in Fig. 5. The mRFP-histone 2B (H2B) fusion protein was prepared using the pSITE-6C1 destination vector. The sequence of all primers and the PCR conditions for mutant preparation are given in Supplementary Table S2 and Supplementary Methods S1, respectively. Plasmids carrying mCherry fused with either the peroxisomal

targeting signal 1 (PTS1, Ser-Lys-Leu) or the first 29 amino acids (aa) of the yeast (*Saccharomyces cerevisiae*) cytochrome c oxidase subunit IV, used to tag mitochondria (Nelson 2007), were purchased from Arabidopsis Biological Resource Center (ABRC, CD3-983 and CD3-991). Transient transformation of *Nicotiana benthamiana* was performed as in Aggarwal et al. (2014).

#### *The influence of light conditions on AtUVR3 subcellular localization.*

Whole *Nicotiana benthamiana* plants with transiently transformed leaves were dark adapted for 16 h, 3 days after transformation. Transformed leaves were detached and put on a water-soaked paper. They were irradiated for 3 h with blue (470 nm) or red (660 nm) LED light of  $50 \mu\text{mol}\cdot\text{m}^{-2}\cdot\text{s}^{-1}$ , or kept in darkness.

#### **Confocal microscopy**

Transiently transformed *N. benthamiana* leaves were observed with the LSM 880 laser scanning microscope (Carl Zeiss, Jena, Germany), using a Plan-Apo 63x, 1.4 NA oil objective. For samples expressing only a GFP-tagged protein, Ar laser line of 488 nm was used for excitation of GFP and chlorophyll. Emission within the range of 493-598 nm was recorded as the green channel, emission in the range of 630-721 nm as the magenta channel. Images of samples expressing both GFP and mCherry/mRFP tagged proteins were recorded in two tracks with separate excitation and emission channels. Tracks were switched every line. In the first track, an Ar laser line of 488 nm was used for excitation of GFP and chlorophyll. Emission within the range of 493-575 nm was recorded as the green channel, emission in the range of 655-721 nm as the magenta channel. In the second track, a DPSS 561 nm laser was used for the excitation of mCherry or mRFP, and emission in the range 614-650 nm was recorded as the red channel. AtUVR3-GFP fluorescence in the nucleus was bright enough to permit image recording with a low gain (typically gain was around 560, pinhole 1 AU and 2% AOTF transmittance). In chloroplasts and mitochondria, fluorescence was less bright, so a higher gain (650 - 700) and wider pinhole (90  $\mu\text{m}$ ) was applied. Cell overviews in figs. 3, 6, 7, S4 and S7 were collected with pinhole set to 90  $\mu\text{m}$ , 2% AOTF transmittance and the gain specified in the figures. Image analysis was performed with ImageJ software.

#### **FUNDING**

This work was supported by the Polish National Science Centre [grant no. UMO-2011/03/D/NZ3/00210]. The research was carried out in part with equipment purchased thanks to the financial support of the European Regional Development Fund in the framework of the Polish Innovation Economy Operational Program [contract no. POIG.02.01.00-12-167/08], project Malopolska Centre of Biotechnology - MCB. Confocal microscopy

analysis was conducted in part in the Laboratory of Imaging and Atomic Force Spectroscopy of MCB. The Faculty of Biochemistry, Biophysics and Biotechnology of Jagiellonian University is the beneficiary of structural funds from the European Union [grant no. POIG.02.01.00-12-064/08]. The Faculty of Biochemistry, Biophysics and Biotechnology is a partner of the Leading National Research Center (KNOW) supported by the Ministry of Science and Higher Education.

#### DISCLOSURES

The authors have no conflicts of interest to declare.

#### REFERENCES:

- Aggarwal, C., Banaś, A.K., Kasprówicz-Maluśki, A., Borghetti, C., Łabuz, J., Dobrucki, J., et al. (2014) Blue-light-activated phototropin2 trafficking from the cytoplasm to Golgi/post-Golgi vesicles. *J. Exp. Bot.* 65: 3263-3276.
- Ahmad, M., Jarillo, J.A., Klimczak, L.J., Landry, L.G., Peng, T., Last, R.L., et al. (1997) An enzyme similar to animal type II photolyase mediates photoreactivation in *Arabidopsis*. *Plant Cell* 9: 199-207.
- Antoniali, G., Lirussi, L., Poletto, M. and Tell, G. (2014) Emerging roles of the nucleolus in regulating the DNA damage response: the noncanonical DNA repair enzyme APE1/Ref-1 as a paradigmatical example. *Antioxid. Redox Signal.* 20: 621-639.
- Armbruster, U., Hertle, A., Makarenko, E., Zühlke, J., Pribil, M., Dietzmann, A., et al. (2009) Chloroplast proteins without cleavable transit peptides: rare exceptions or a major constituent of the chloroplast proteome? *Mol. Plant* 2: 1325-1335.
- Brameier, M., Krings, A. and Maccallum, R.M. (2007) NucPred - Predicting Nuclear Localization of Proteins. *Bioinformatics* 23: 1159-1160.
- Brown, J.W., Shaw, P.J., Shaw, P. and Marshall, D.F. (2005) *Arabidopsis* nucleolar protein database (AtNoPDB). *Nucleic Acids Res.* 33: 633-636.
- Bucher, D.B., Pilles, B.M., Carell, T. and Zinth, W. (2015) Dewar lesion formation in single- and double-stranded DNA is quenched by neighboring bases. *J. Phys. Chem. B* 119: 8685-8692.
- Castells, E., Molinier, J., Drevensek, S., Genschik, P., Barneche, F. and Bowler, C. (2010) *Det1-1*-induced UV-C hyposensitivity through *UVR3* and *PHR1* photolyase gene over-expression. *Plant J.* 63: 392-404.

- Chaudhari, V.R., Vyawahare, A., Bhattacharjee, S.K. and Rao, B.J. (2015) Enhanced excision repair and lack of PSII activity contribute to higher UV survival of *Chlamydomonas reinhardtii* cells in dark. *Plant Physiol. Bioch.* 88: 60–69.
- Chen, J.-J., Jiang, C.-Z. and Britt, A.B. (1996) Little or no repair of cyclobutane pyrimidine dimers is observed in the organellar genome of the young *Arabidopsis* seedling. *Plant Physiol.* 111: 19–25.
- la Cour, T., Kiemer, L., Mølgaard, A., Gupta, R., Skriver, K. and Brunak, S. (2004) Analysis and prediction of leucine-rich nuclear export signals. *Protein Eng. Des. Sel.* 17: 527–536.
- Crivelli, G., Ciuffo, M., Genre, A., Masenga, V. and Turina, M. (2011) Reverse genetic analysis of ourmiaviruses reveals the nucleolar localization of the coat protein in *Nicotiana benthamiana* and unusual requirements for virion formation. *J. Virol.* 85: 5091–5104.
- Czechowski, T., Stitt, M., Altmann, T., Udvardi, M.K. and Scheible, W.R. (2005) Genome-wide identification and testing of superior reference genes for transcript normalization in *Arabidopsis*. *Plant Physiol.* 139: 5–17.
- Devlin, P.F., Yanovsky, M.J. and Kay, S.A. (2003) A genomic analysis of the shade avoidance response in *Arabidopsis*. *Plant Physiol.* 133: 1617–1629.
- Draper, C.K. and Hays, J.B. (2000) Replication of chloroplast, mitochondrial and nuclear DNA during growth of unirradiated and UVB-irradiated *Arabidopsis* leaves. *Plant J.* 23: 255–265.
- Favory, J.J., Stec, A., Gruber, H., Rizzini, L., Oravecz, A., Funk M., et al. (2009) Interaction of COP1 and UVR8 regulates UV-B-induced photomorphogenesis and stress acclimation in *Arabidopsis*. *EMBO J.* 28: 591–601.
- Friedberg, E.C., Walker, G.C. and Siede, W. (1995) DNA Repair and Mutagenesis. Washington, DC: ASM Press.
- Gushchin, V.A., Lukhovitskaya, N.I., Andreev, D.E., Wright, K.M., Taliansky, M.E., Solovyev, A.G., et al. (2013) Dynamic localization of two tobamovirus ORF6 proteins involves distinct organellar compartments. *J. Gen. Virol.* 94: 230–240.
- Hitomi, K., DiTacchio, L., Arvai, A.S., Yamamoto, J., Kim, S.T. Todo, T., et al. (2009) Functional motifs in the (6-4) photolyase crystal structure make a comparative framework for DNA repair photolyases and clock cryptochromes. *Proc. Natl Acad Sci. USA*, 106(17): 6962–6967.
- Hudson, M.E. and Quail, P.H. (2003). Identification of promoter motifs involved in the network of phytochrome A-regulated gene expression by combined analysis of genomic sequence and microarray data. *Plant Physiol.* 133: 1605–1616.

- Jarvis, P. (2008) Targeting of nucleus-encoded proteins to chloroplasts in plants. *New Phytol.* 179: 257-285.
- Jiang, C.-Z., Yee, J. Mitchell, D.L. and Britt, A.B. (1997) Photorepair mutants of *Arabidopsis*. *Proc. Natl Acad Sci. USA*, 94: 7441–7445.
- Kaiser, G. Kleiner, O., Beisswenger, C. and Batschauer, A. (2009) Increased DNA repair in *Arabidopsis* plants overexpressing CPD photolyase. *Planta* 230: 505–515.
- Kleine, T., Lockhart, P. and Batschauer, A. (2003) An *Arabidopsis* protein closely related to *Synechocystis* cryptochrome is targeted to organelles. *Plant J.* 35: 8193–9103.
- Kosugi, S., Hasebe, M., Tomita, M. and Yanagawa, H. (2009) Systematic identification of yeast cell cycle-dependent nucleocytoplasmic shuttling proteins by prediction of composite motifs. *Proc. Natl. Acad. Sci. USA* 106: 10171-10176.
- Łabuz, J., Sztatelman, O., Banaś, A.K., and Gabryś, H. (2012) Expression of phototropins in *Arabidopsis* leaves: developmental and light regulation. *J. Exp. Bot.* 63: 1763-1771.
- Lehmann, P., Nöthen, J., von Braun, S.S., Bohnsack, M.T., Mirus, O. and Schleiff, E. (2011) Transitions of gene expression induced by short-term blue light. *Plant Biology* 13: 349–361.
- Lepage, E., Zampini, E. and Brisson, N. (2013) Plastid genome instability leads to reactive oxygen species production and plastid-to-nucleus retrograde signaling in *Arabidopsis*. *Plant Physiol.* 163: 867-881.
- Li, N., Teranishi, M., Yamaguchi, H., Matsushita, T., Watahiki, M.K., Tsuge, T., Li, S.-S. and Hidema, J. (2015) UV-B-induced CPD photolyase gene expression is regulated by UVR8-dependent and -independent pathways in *Arabidopsis*. *Plant Cell Physiol.* 56: 2014-2023.
- Liu, Z., Hossain, G.S., Islas-Osuna, M.A., Mitchell, D.L. and Mount, D.W. (2000) Repair of UV damage in plants by nucleotide excision repair: Arabidopsis UVH1 DNA repair gene is a homologue of *Saccharomyces cerevisiae* Rad1. *Plant J.* 21: 519–528.
- Martin, K., Kopperud, K., Chakrabarty, R., Banerjee, R., Brooks, R. and Goodin, M.M. (2009). Transient expression in *Nicotiana benthamiana* fluorescent marker lines provides enhanced definition of protein localization, movement and interactions in planta. *Plant J.* 59: 150-162.
- Martín, G., Leivar, P., Ludevid, D., Tepperman, J.M., Quail, P.H. and Monte E. (2016) Phytochrome and retrograde signalling pathways converge to antagonistically regulate a light-induced transcriptional network. *Nat. Commun.* 7:11431.
- Moldt, J., Pokorný, R., Orth, C., Linne, U., Geisselbrecht, Y., Marahiel, M.A., et al. (2009) Photoreduction of the folate cofactor in members of the photolyase family. *J. Biol. Chem.* 284: 2167-21683.

- Musinova, Y.R., Kananykhina, E.Y., Potashnikova, D.M., Lisitsyna, O.M. and Sheval, E.V. (2015) A charge-dependent mechanism is responsible for the dynamic accumulation of proteins inside nucleoli. *Biochim. Biophys. Acta* 1853: 101-110.
- Nakajima, S., Sugiyama, M., Iwai, S., Hitomi, K., Otsoshi, K., Kim, S.-T., et al. (1998) Cloning and characterization of a gene (UVR3) required for photorepair of 6-4 photoproducts in *Arabidopsis thaliana*. *Nucleic Acids Res.* 26: 638-644.
- Nelson, B., Cai, X. and Nebenführ, A. (2007) A multicolored set of in vivo organelle markers for co-localization studies in *Arabidopsis* and other plants. *Plant J.* 51: 1126-1136.
- Ogawa, L.M., and Baserga, S.J. (2017) Crosstalk between the nucleolus and the DNA damage response. *Mol. BioSyst.* 13: 443-455.
- Pendle, A.F., Clark, G.P., Boon, R., Lewandowska, D., Lam, Y.W., Andersen, J., et al. (2005) Proteomic analysis of the *Arabidopsis* nucleolus suggests novel nucleolar functions. *Mol. Biol Cell* 16: 260-269.
- Petrucchio, S., Volpi, G., Bolchi, A., Rivetti, C. and Ottonello, S. (2002) A nick-sensing DNA 3'-repair enzyme from *Arabidopsis*. *J. Biol. Chem.* 277: 23675-23683.
- Pokorny, R., Klar, T., Hennecke, U., Carell, T., Batschauer, A. and Essen, L.-O. (2008) Recognition and repair of UV lesions in loop structures of duplex DNA by DASH-type cryptochrome. *Proc. Natl Acad. Sci. USA* 105: 21023–21027.
- Porollo, A. and Meller, J. (2007) Versatile annotation and publication quality visualization of protein complexes using POLYVIEW-3D, *BMC Bioinformatics*, 8: 316.
- Rastogi, R.P., Richa, Kumar, A., Tyagi, M.B. and Sinha, R.P. (2010) Molecular mechanisms of ultraviolet radiation-induced DNA damage and repair. *J. Nucleic Acids* 2010: 592980
- Rossi, M., Genre, A. and Turina, M. (2014) Genetic dissection of a putative nucleolar localization signal in the coat protein of ourmia melon virus. *Arch. Virol.* 159: 1187-1192.
- Selby, C.P. and Sancar, A. (2006) A cryptochrome/photolyase class of enzymes with single-stranded DNA-specific photolyase activity. *Proc. Natl Acad. Sci. USA* 103: 17696–17700.
- Sztatelman, O., Grzyb, J., Gabryś, H. and Banaś, A.K. (2015) The effect of UV-B on *Arabidopsis* leaves depends on light conditions after treatment. *BMC Plant Biol.* 15: 281.
- Takahashi, M., Teranishi, M., Ishida, H., Kawasaki, J., Takeuchi, A., Yamaya, T., et al. (2011) Cyclobutane pyrimidine dimer (CPD) photolyase repairs ultraviolet-B-induced CPDs in rice chloroplast and mitochondrial DNA. *Plant Journal* 66: 433–442.

- Takahashi, S., Teranishi, M., Izumi, M., Takahashi, M., Takahashi, F. and Hidema, J. (2014) Transport of rice cyclobutane pyrimidine dimer photolyase into mitochondria relies on a targeting sequence located in its C-terminal internal region. *Plant J.* 79: 951-963.
- Tanaka, A., Sakamoto, A., Ishigaki, Y., Nikaido, O., Sun, G., Hase Y., et al. (2002) An Ultraviolet-B-Resistant mutant with enhanced DNA repair in *Arabidopsis*. *Plant Physiol.* 129: 64-71.
- Tanz, S.K., Castleden, I., Hooper, C.M., Vacher, M., Small, I. and Millar, A.H. (2013) SUBA3: a database for integrating experimentation and prediction to define the SUBcellular location of proteins in *Arabidopsis*. *Nucleic Acids Res.* 41: D1185-91
- Valverde, F., Mouradov, A., Soppe, W., Ravenscroft, D., Samach, A. and Coupland, G. (2004) Photoreceptor regulation of CONSTANS protein in photoperiodic flowering. *Science* 303(5660): 1003-6.
- Vandesompele, J., de Preter, K., Pattyn, F., Poppe, B., van Roy, N., de Paepe, A. and Speleman, F. (2002) Accurate normalization of real-time quantitative RT-PCR data by geometric averaging of multiple internal control genes. *Genome Biol.* 3: RESEARCH0034.
- Waterworth, W.M., Jiang, Q., West, C.E., Nikaido, M. and Bray, C.M. (2002) Characterization of *Arabidopsis* photolyase enzymes and analysis of their role in protection from ultraviolet-B radiation. *J. Exp. Bot.* 53: 1005-1015.
- Waterworth, W.M., Drury, G.E., Bray, C.M. and West, C.E. (2011) Repairing breaks in the plant genome: the importance of keeping it together. *New Phytol.* 192: 805-822.
- Whitelam, G.C., Johnson, E., Peng, J., Carol, P., Anderson, M.L., Cowl, J.S. and Harberd, N.P. (1993) Phytochrome A null mutants of *Arabidopsis* display a wild-type phenotype in white light. *Plant Cell* 5(7): 757-768.
- Wege, S., Khan, G.A., Jung, J.Y., Vogiatzaki, E., Pradervand, S., Aller, I., et al. (2016). The EXS domain of PHO1 participates in the response of shoots to phosphate deficiency via a root-to-shoot signal. *Plant Physiol.* 170: 385-400.

#### FIGURE LEGENDS

**Fig. 1.** The expression of *AtUVR3*. (A) The expression of *AtUVR3* in *Arabidopsis* roots, stems, flowers and siliques, from soil grown plants in the middle of the day. (B) Effect of UVB on *AtUVR3* mRNA level. 5-week-old WT or *uvr8-6* plants were dark-adapted and irradiated for 3 h with UVB ( $0.2 \mu\text{mol}\cdot\text{m}^{-2}\cdot\text{s}^{-1}$ ) or kept in

darkness (dark). (C) The effect of white light on *AtUVR3* expression in green parts of seedlings and in mature leaves. Seedlings and whole 5-week old plants were dark-adapted and illuminated for 3 h with white light ( $100 \mu\text{mol}\cdot\text{m}^{-2}\cdot\text{s}^{-1}$ ) or left in darkness (dark). (D) The impact of DCMU on *AtUVR3* transcript levels. 5-week-old plants were treated with 200  $\mu\text{M}$  DCMU in 0.4% DMSO or in only 0.4% DMSO (control). The plants were dark-adapted and illuminated for 3 h with white light ( $200 \mu\text{mol}\cdot\text{m}^{-2}\cdot\text{s}^{-1}$ ) or left in darkness. Each bar corresponds to an average of three biological replicates. Each replicate consisted of samples pooled from different plants. Error bars - SE. Asterisks indicate statistically significant differences between illuminated and dark-adapted samples (\*  $p$  0.01–0.05; \*\*  $p$  0.001–0.01, \*\*\*  $p$  < 0.001, calculated with the Student's t test in B-D). The differences between means in A were insignificant when tested with Tukey's test.

**Fig. 2.** The effect of blue and red light on the mRNA level of *AtUVR3* in (A) mature leaves and (B) 7-day-old seedlings of wild type *Arabidopsis* and photoreceptor mutants. 5-week-old soil-grown plants and light-grown seedlings were dark-adapted. Whole plants and seedlings (etiolated and light-grown) were illuminated for 3 h with red or blue light ( $50 \mu\text{mol}\cdot\text{m}^{-2}\cdot\text{s}^{-1}$ ) or left in darkness. Each bar corresponds to an average of three biological replicates. Error bars – SE. Asterisks indicate statistically significant differences between illuminated and dark-adapted samples, treated as controls (\*  $p$  0.01–0.05; \*\*  $p$  0.001–0.01, \*\*\*  $p$  < 0.001, calculated with the Dunnett's test).

**Fig. 3.** Subcellular localization of *AtUVR3*-GFP in the epidermis of transiently transformed *N. benthamiana* leaves. Localization of *AtUVR3*-GFP (A) in the nucleus, (B) in mitochondria and (C) in chloroplasts. (D) Images of epidermal cells expressing *AtUVR3*-GFP and empty GFP (pK7FWG2) collected with different gains. *AtUVR3*-GFP is present mainly in nuclei, while empty GFP is present both in the cytoplasm and the nucleus. GFP fluorescence in green, chlorophyll autofluorescence in magenta.

**Fig. 4.** Subcellular localization of *AtUVR3*-GFP co-expressed with (A) histone H2B tagged with mRFP, (B) mCherry fused with the first 29 aa of the yeast cytochrome c oxidase subunit IV used to label mitochondria, (C) PTS1-mCherry, a peroxisome marker. *AtUVR3*-GFP co-localizes with mitochondria but not with peroxisomes. GFP fluorescence in green, mRFP and mCherry fluorescence in red.

**Fig. 5.** The structure of (A) muteins and (B) truncated AtUVR3 proteins. (A) Amino acid (aa) sequence of AtUVR3. Putative nuclear localization signals (pNLSs) are in grey boxes, putative nuclear export signals (NES) are in black boxes. The bipartite NLS is underlined. White letters in grey boxes (m1 - m4) represent K and R residues substituted with A in muteins. (B) Truncated AtUVR3 proteins. Gray rectangles correspond to AtUVR3 sequences that were retained in the truncated form, while black lines mark the removed sequences. Full length (556 aa) AtUVR3 contains 3 putative NLS sequences marked as pNLS1 to pNLS3 in (A).

**Fig. 6.** Subcellular localization of AtUVR3<sub>(1-501)</sub>-GFP (AtUVR3 without the C-terminal helix) in the epidermis of transiently transformed *N. benthamiana* leaves. (A) AtUVR3<sub>(1-501)</sub>-GFP is localized in the nucleoplasm but not in the nucleolus. Intensity of green fluorescence is similar in the nucleus and the surrounding cytoplasm. (B) AtUVR3<sub>(1-501)</sub>-GFP is present in mitochondria. (C) Mitochondrial localization of AtUVR3<sub>(1-501)</sub>-GFP was confirmed by co-transformation with mCherry fused with the first 29 aa of the yeast cytochrome c oxidase subunit IV. (D) The concentration of AtUVR3<sub>(1-501)</sub>-GFP in chloroplasts is lower than in the surrounding cytoplasm. (E) Images of epidermal cells expressing AtUVR3<sub>(1-501)</sub>-GFP, collected with increasing gain. GFP fluorescence in green, mCherry fluorescence in red, chlorophyll autofluorescence in magenta.

**Fig. 7.** Subcellular localization of AtUVR3<sub>(122-556)</sub>-GFP (AtUVR3 without the N-terminal part) in the epidermis of transiently transformed *N. benthamiana* leaves. (A) AtUVR3<sub>(122-556)</sub>-GFP is localized in the nucleoplasm (with clear retention in the nucleolus). (B) AtUVR3<sub>(122-556)</sub>-GFP is also present in mitochondria. (C) Mitochondrial localization of AtUVR3<sub>(122-556)</sub>-GFP was confirmed by co-transformation with mCherry, fused with the first 29 aa of the yeast cytochrome c oxidase subunit IV used to label mitochondria. (D) AtUVR3<sub>(122-556)</sub>-GFP is present in chloroplasts. (E) Images of epidermal cells expressing AtUVR3<sub>(122-556)</sub>-GFP, collected with increasing gain. GFP fluorescence in green, mCherry fluorescence in red, chlorophyll autofluorescence in magenta.

**Fig. 8.** The effect of amino acids substitution on the sub-nuclear localization of AtUVR3. Lysine or arginine residues in positions 122, 124-125 (m1), 509-511 (m2), 520-521 (m3), 535-537 (m4) were substituted with alanine residues in muteins fused with GFP. Nuclei were imaged in the epidermal cells of transiently transformed *N. benthamiana* leaves. GFP fluorescence in green, chlorophyll autofluorescence in magenta.

**Fig. 9.** The effect of amino acids substitution on chloroplast localization of AtUVR3. Lysine or arginine residues in positions 122, 124-125 (m1), 509-511 (m2), 520-521 (m3), 535-537 (m4) were substituted with alanine residues in muteins fused with GFP. Chloroplasts were imaged in the epidermal cells of transiently transformed *N. benthamiana* leaves. GFP fluorescence in green, chlorophyll autofluorescence in magenta.

**Fig. 10.** The effect of amino acid substitution on mitochondrial localization of AtUVR3. Lysine or arginine residues in positions 122, 124-125 (m1), 509-511 (m2), 520-521 (m3), 535-537 (m4) were substituted with alanine residues. Muteins fused with GFP were co-expressed with mCherry fused to the N-terminal sequence of cytochrome c-oxidase subunit IV in the epidermis of transiently transformed *N. benthamiana* leaves. GFP fluorescence in green, mCherry fluorescence in red.

For Peer Review

## SUPPLEMENTARY DATA

**Supplementary Methods S1.** PCR conditions for *AtUVR3* mutagenesis.

**Supplementary Table S1.** The list of primers used for real-time PCR.

**Supplementary Table S2.** The list of primers used in gateway cloning and for preparation of *AtUVR3* muteins.

**Supplementary Figure S1.** The effect of (A) the intensity of white light applied for 3 h and (B) duration of illumination with  $100 \mu\text{mol}\cdot\text{m}^{-2}\cdot\text{s}^{-1}$  white light on the mRNA level of *AtUVR3* in mature *Arabidopsis* leaves. Each point corresponds to a single biological replicate, consisting of leaves pooled from 10 plants.

**Supplementary Figure S2.** The effect of blue and red light on the mRNA level of *AtUVR3* in the mature leaves of wild type (*Ler*) and phytochrome (*phyA*, *phyB*, *phyAB*) mutants (*Ler* background) of *Arabidopsis*. 5-week-old plants were dark adapted and illuminated with  $50 \mu\text{mol}\cdot\text{m}^{-2}\cdot\text{s}^{-1}$  of blue or red light for 3 h or left in darkness.

**Supplementary Figure S3.** The sub-nuclear localization of the GFP protein (pK7FWG2). GFP fluorescence is localized uniformly in the nucleoplasm and is not observed in the nucleolus. GFP is also present in the cytoplasm surrounding the nucleus, but it is absent from chloroplasts and mitochondria, labeled with mCherry fused to the N-terminal sequence of cytochrome c-oxidase subunit IV. GFP fluorescence in green, mCherry – red, chlorophyll autofluorescence in magenta.

**Supplementary Figure S4.** The subcellular localization of *AtUVR3*-GFP under different light conditions. Three days after transformation whole *Nicotiana* plants were dark adapted. Detached leaves were illuminated for 3 h with  $50 \mu\text{mol}\cdot\text{m}^{-2}\cdot\text{s}^{-1}$  of red or blue light or left in darkness. GFP fluorescence in green, chlorophyll autofluorescence in magenta.

**Supplementary Figure S5.** The *AtUVR3* protein model. (A) The *AtUVR3* protein model rendered using PyMol. The protein chain was rendered as a cartoon, ligands as balls and sticks. The amino acids substituted in muteins were depicted as sticks and highlighted with colours (m1 in yellow, m2 in red, m3 in blue and m4 in green). (B) A space fill view of *AtUVR3* protein. Hydrophobic residues (A, C, F, G, I, L, M, P, V) are in yellow; amphipathic (H, W, Y) - dark yellow; polar (N, Q, S, T) - orange; negatively charged (D, E) - red; positively charged (R, K) - brown.

**Supplementary Figure S6.** Epidermal cells of *N. benthamiana* co-expressing *AtUVR3* muteins fused with GFP and mCherry fused to the N-terminal sequence of cytochrome c-oxidase subunit IV (a mitochondrial marker). GFP fluorescence in green, mCherry in red.

**Supplementary Figure S7.** Images of *N. benthamiana* epidermal cells expressing AtUVR3 muteins fused with GFP collected with increasing gain. Muteins .m1, .m2 and .m3 are efficiently transported into nuclei (similar to the wild type AtUVR3-GFP). .m4 and all double/triple muteins are clearly visible in the cytoplasm. GFP fluorescence in red, chlorophyll autofluorescence in magenta.

For Peer Review

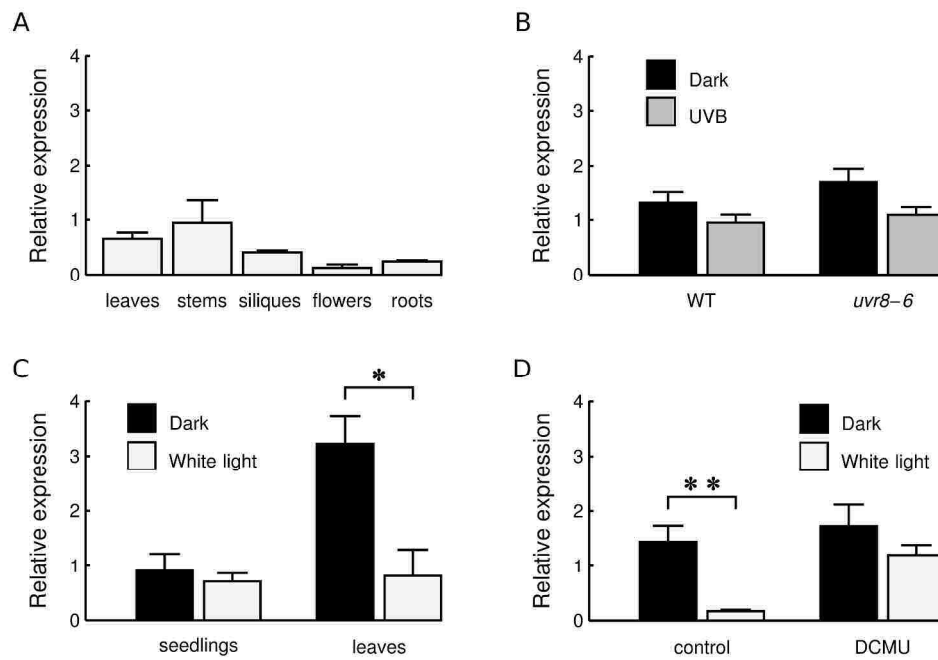


Figure 1

124x81mm (600 x 600 DPI)

Review

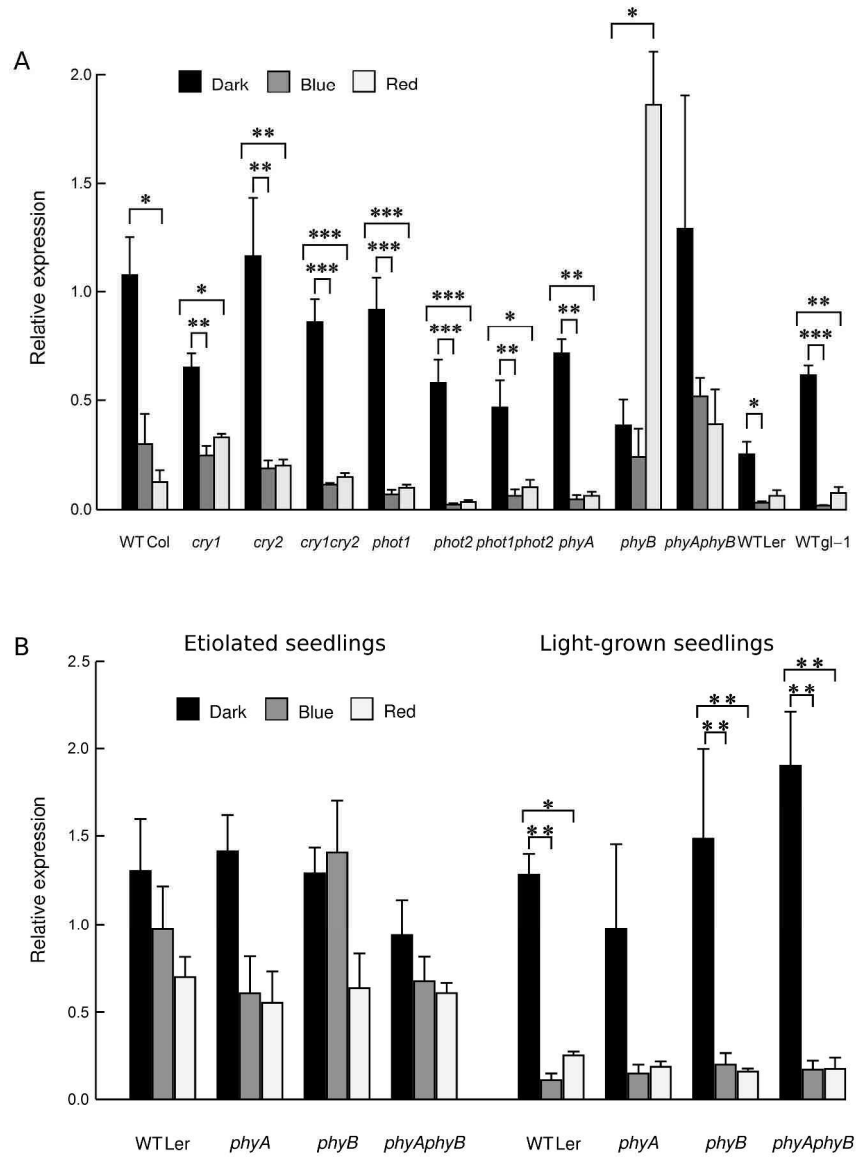


Figure 2

256x346mm (600 x 600 DPI)

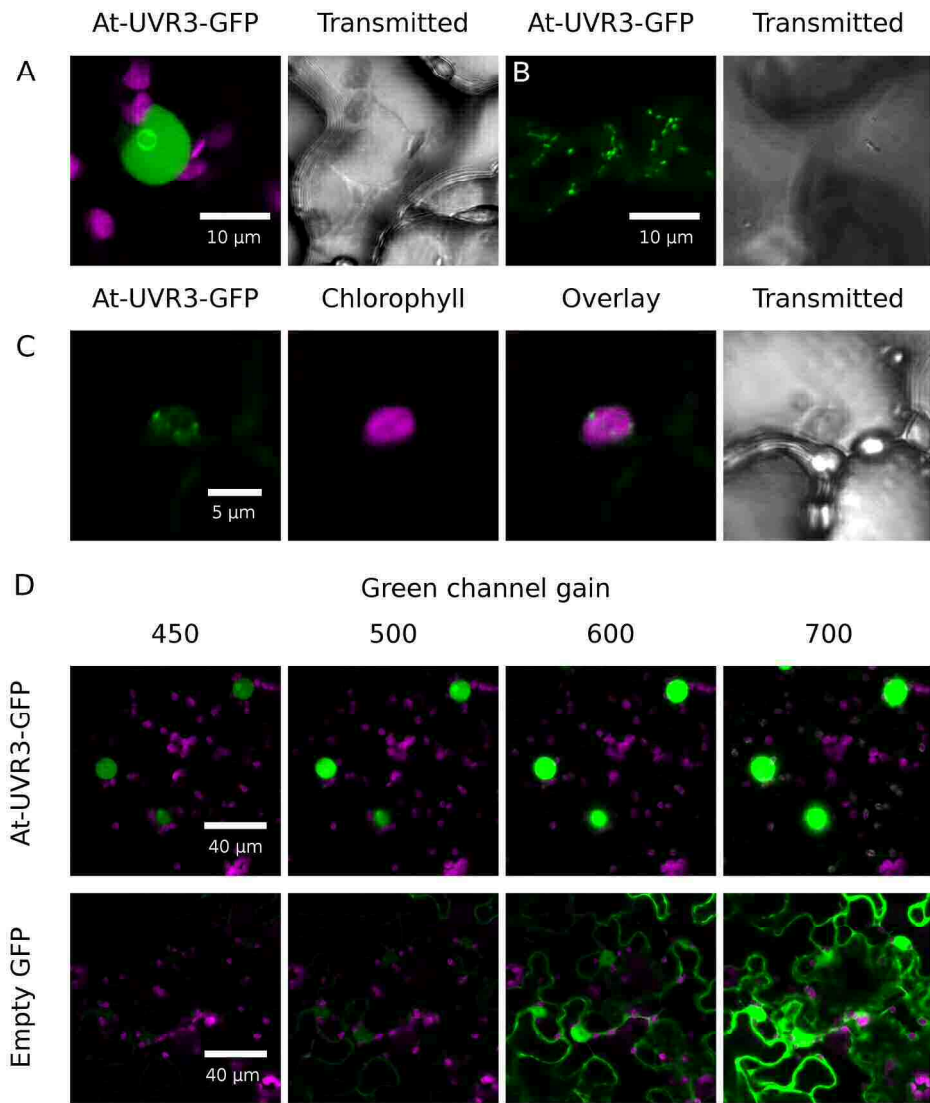


Figure 3

209x245mm (300 x 300 DPI)

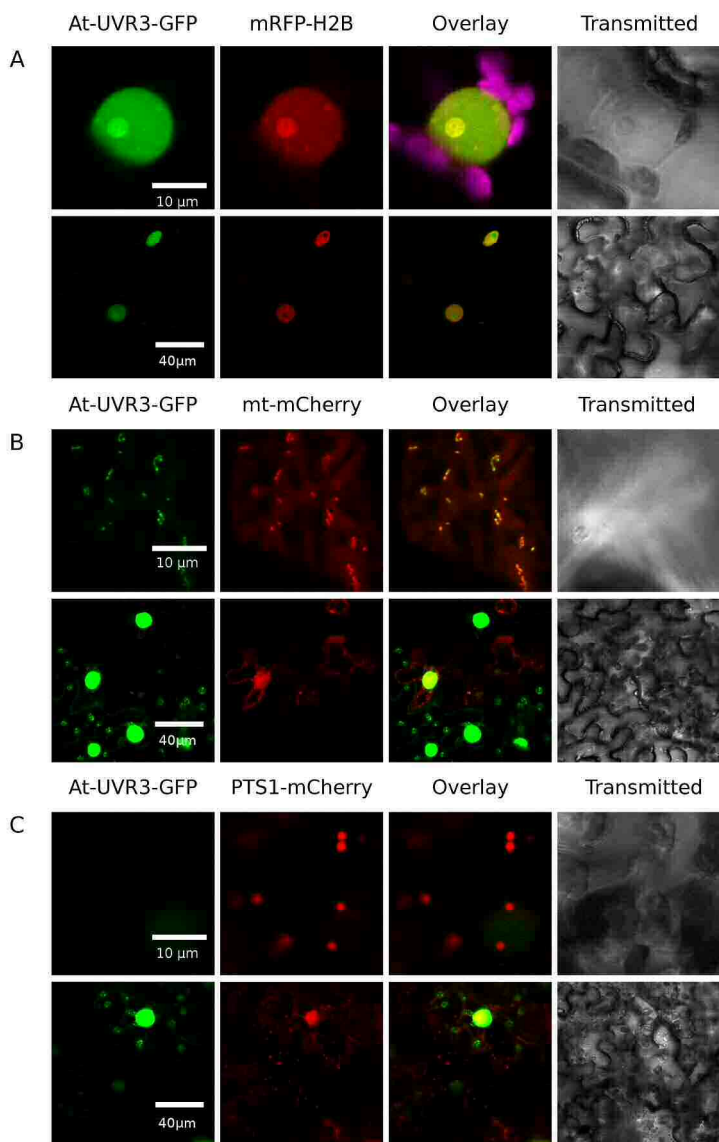


Figure 4

278x433mm (300 x 300 DPI)

**A**

```

1  MQRFCVCSPPSSYRLNPIITSMATGSGSLIWFFRKGLRVHDNPALEYASKGSE 50
51  FMYPVFVIDPHYMESDPSAFSPGSSRAGVNRIRFLLESSLKDLDSSLKKLG 100
      m1
101 SRLLVFKGEPGEVLVRCIQEWVKFLCFEYDTPYYQALDVKVKDYASST 150
151  GVEVFSSPVSHTLFNPAHIIKNGGKPPLSYQSFLKVAGEPSCAKSELVMS 200
201  YSSLPPIGDIGNLGISEVPSLEELGYKDDEQADWTPFRGGESEALKRLTK 250
251  SISKAWVANFEKPKGDPSAFLKPATTVMSPYLKFGCLSSRYFYQCLQNI 300
301  YKDVKKHTSPPVSLGQLLWREFFYTTAFGTPNFDKMKGNRICKQIPWNE 350
351  DHAMLAAWRDGKTGYPWIDAIMVQLLKWGMHHLARHCVACFLTRGDLFI 400
401  HWEQGRDVFERLLIDSDWAINNGHWWLSCSSFFYQFNRIYSPISFGKKY 450
451  DPDGKYIRHFLPVLKDMPKQYIYEPWTAPLSVQTKANCIVGKDYPKPMVL 500
      m2      m3      m4
501  HDSASKECKRFMGEAYALNKIMDGKVDEENLRDLRRFLQKDEHEESKIRN 550
551  QRPKLK
    
```

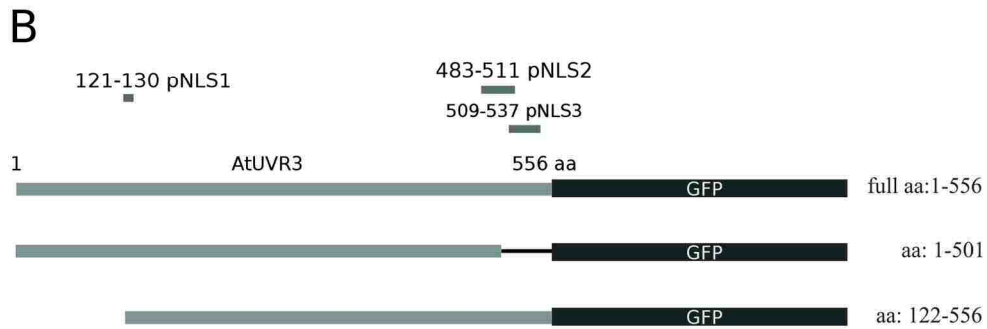


Figure 5

193x207mm (300 x 300 DPI)

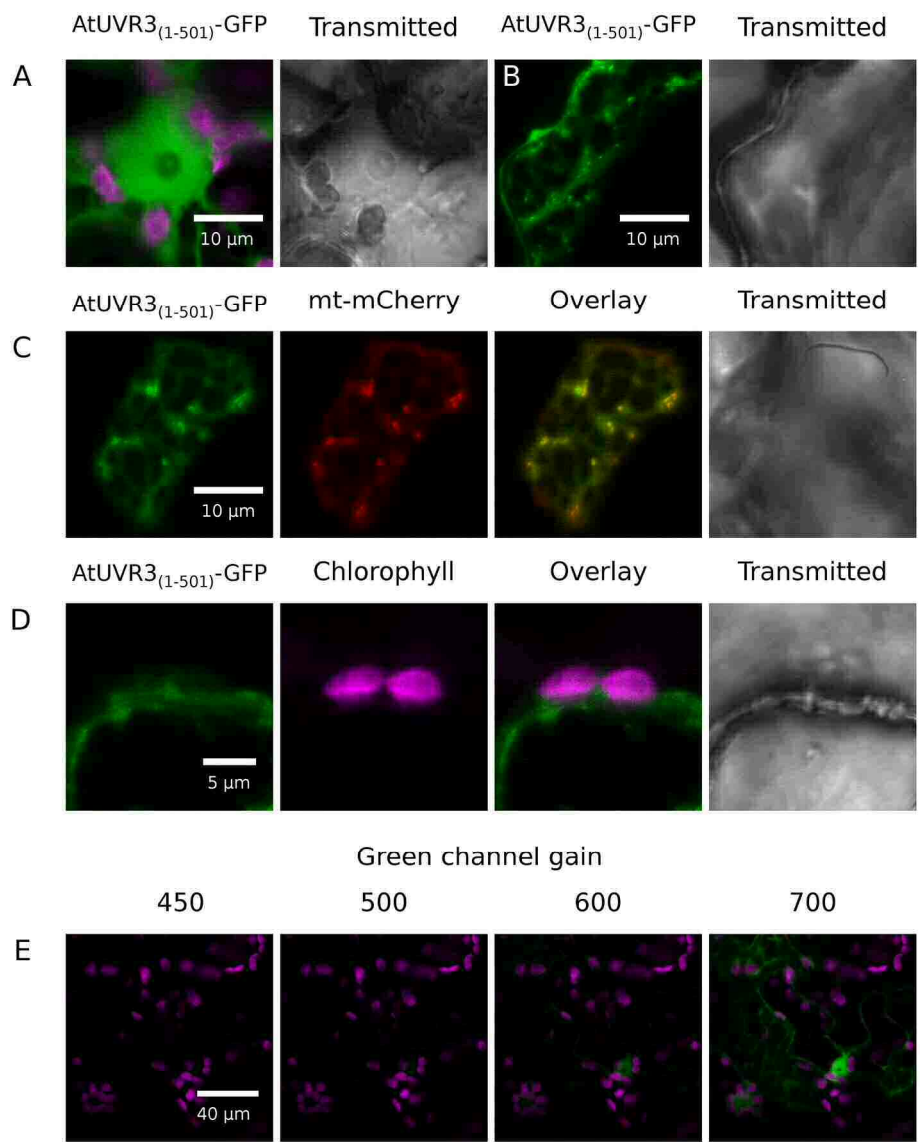


Figure 6

179x224mm (300 x 300 DPI)

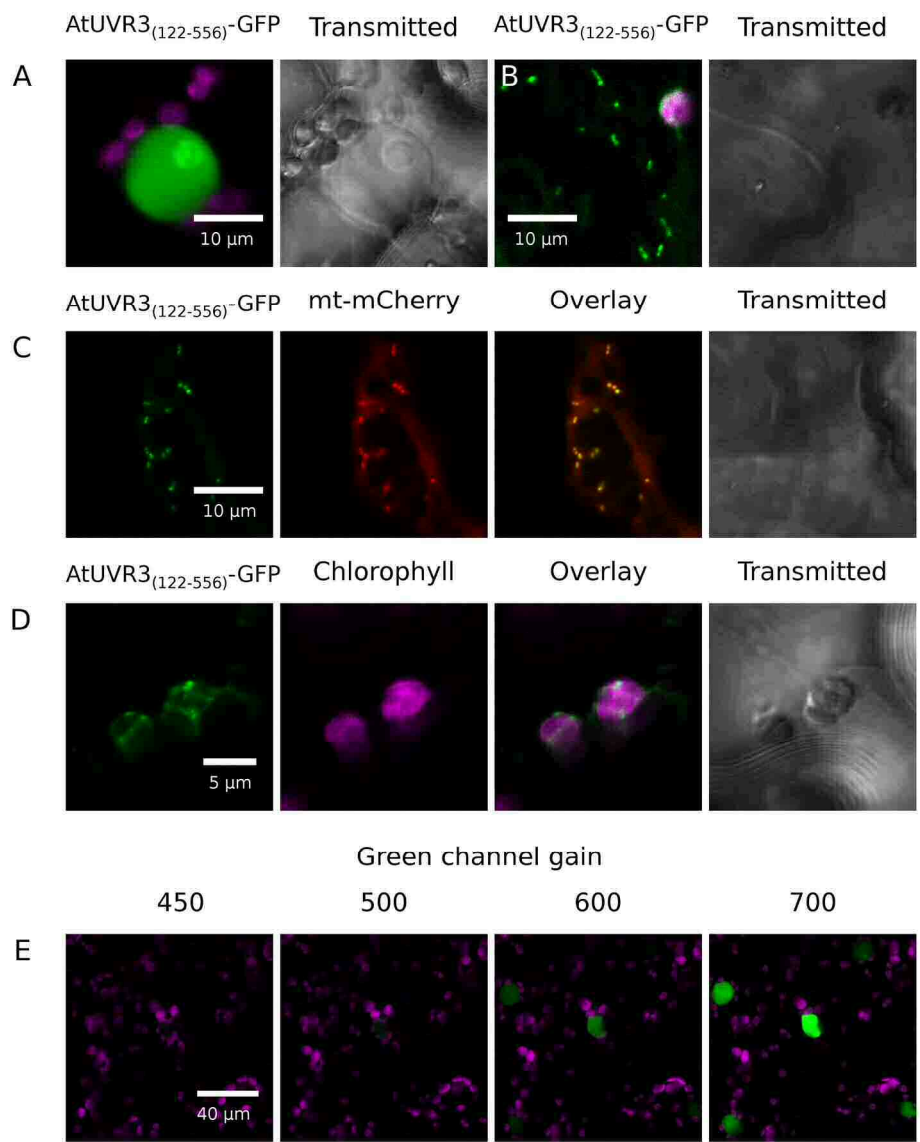


Figure 7

179x224mm (300 x 300 DPI)

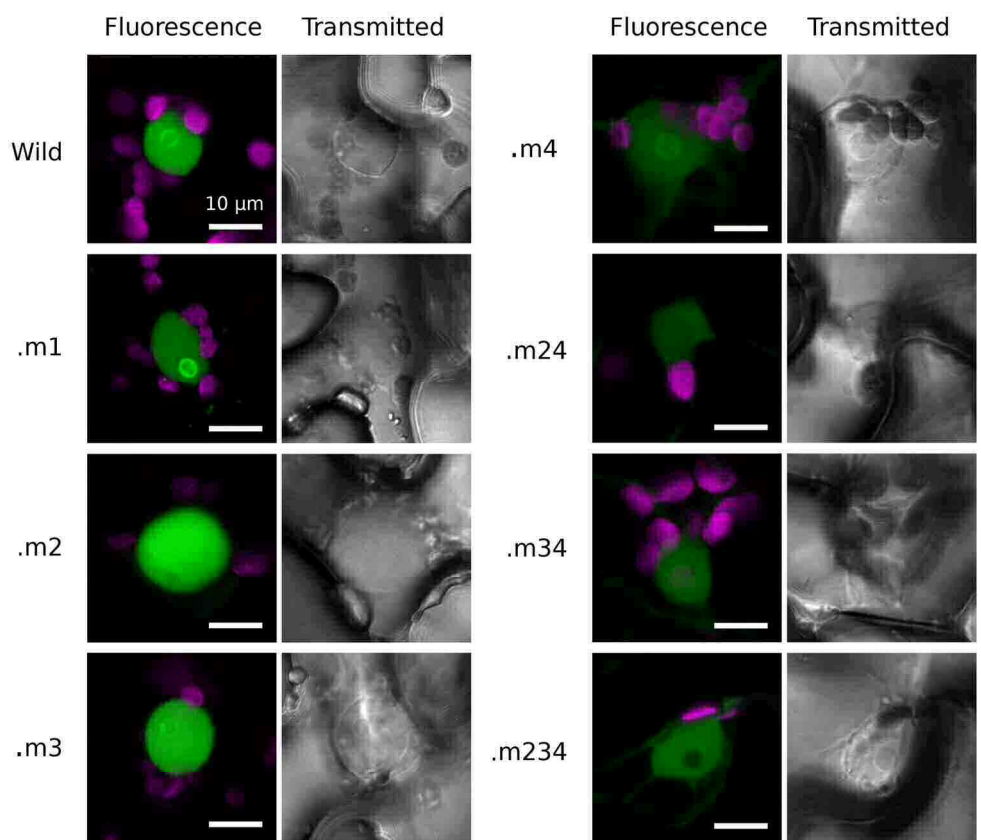


Figure 8

154x136mm (300 x 300 DPI)

ew

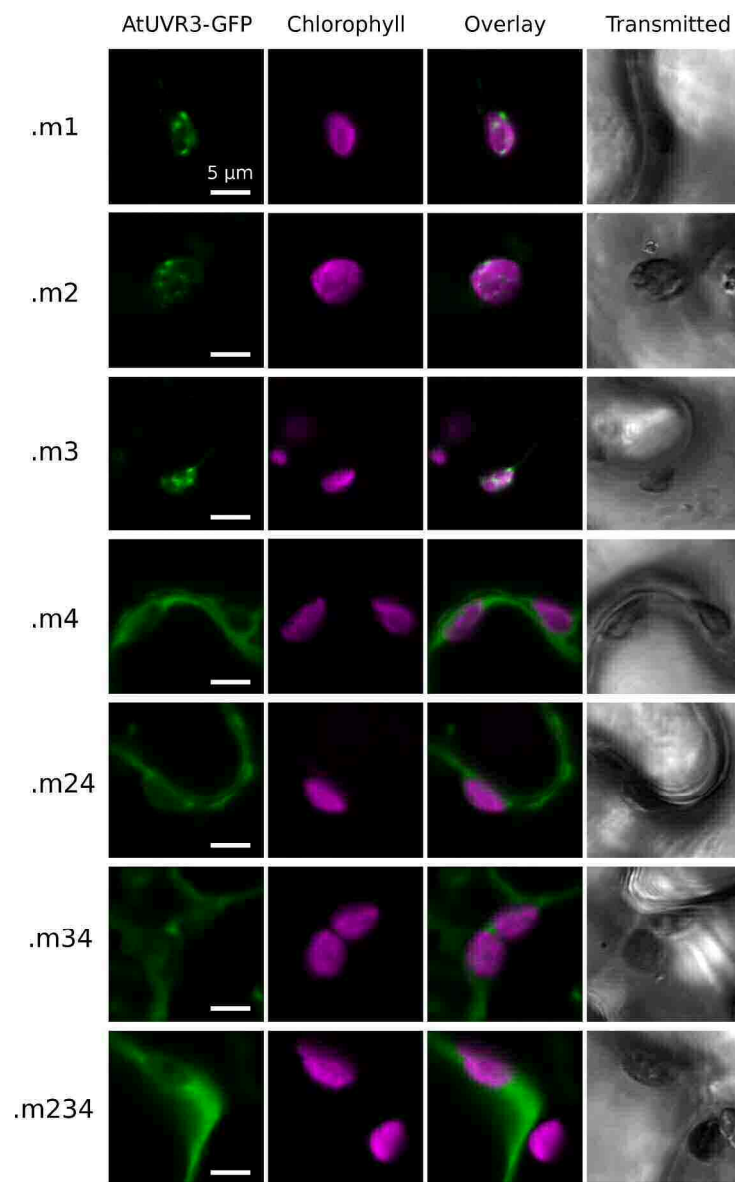


Figure 9

143x228mm (600 x 600 DPI)

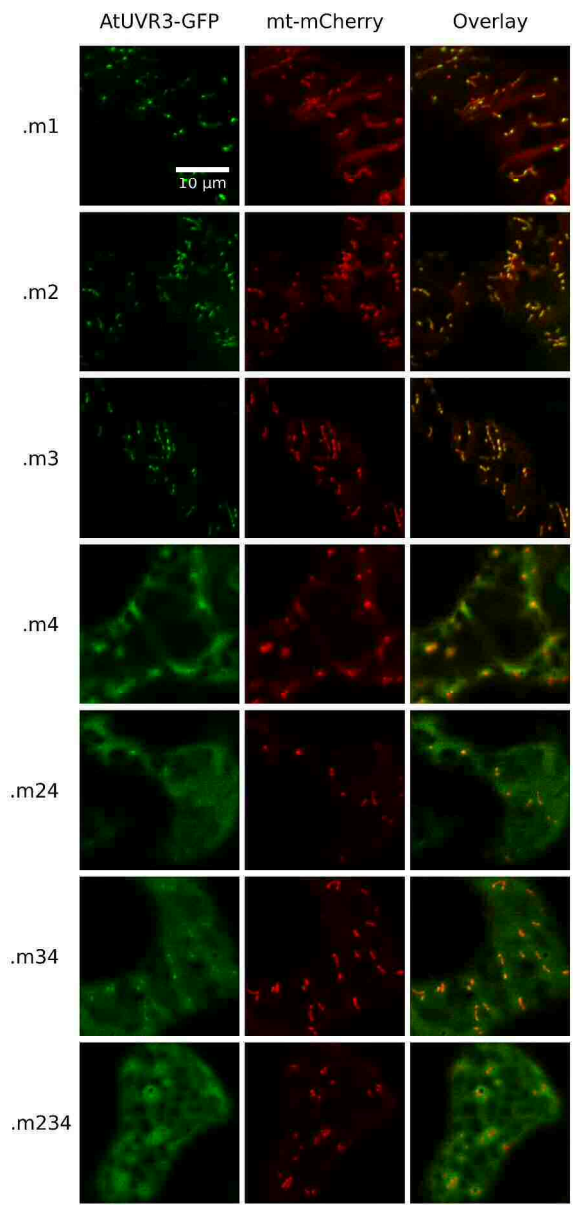


Image 10

229x472mm (600 x 600 DPI)